

# Some theoretical aspects of the two-level magnetovariational method

Massimo Vellante

*Dipartimento di Fisica, Università dell'Aquila, Italy*

## Abstract

We discuss some theoretical aspects of the two-level magnetovariational method for the determination of the underground electrical structure. The properties of two new apparent resistivity functions, respectively depending on gain and phase of the transfer function of the horizontal magnetic field variations between the Earth's surface and a given depth, are examined for two-layer Earth models. The effects of a finite wavelength of the source field are also investigated. It is shown that the measurement of the attenuation of the magnetic vertical component generated by an inhomogeneous source field can provide further information on the vertical distribution of the Earth's conductivity. In particular, it is shown that the measurement of the transfer function of both vertical and horizontal components between two levels can be used to estimate the average conductivity of the interlying medium.

**Key words** *electromagnetic sounding – two-level magnetovariational method – source field effects*

## 1. Introduction

As originally suggested by Berdichevskii and Vanyan (1969), measurement of magnetic field variations at two distinct depths may be an alternative to the standard magnetotelluric method (Kaufman and Keller, 1981) for investigating the electrical structure of the Earth. For instance, this technique has been adopted for studying the conductivity distribution beneath oceans (Poehls and von Herzen, 1976; Law and Greenhouse, 1981; Edwards *et al.*, 1988): in practice, given the conductivity of sea water, in these experiments the electric field in the ocean layer is estimated by measur-

ing the attenuation of the sea floor horizontal magnetic field with respect to the surface.

Two-level magnetovariational measurements have been also conducted by using deep mines (Hardam, 1974; Babour and Mosnier, 1980; Meyer, 1986; review by Schmucker, unpublished report, 1985). In these experiments the vertical separation between surface and underground site ranged between 600 m and 1000 m, and the magnetic field variations were analyzed in the frequency range of micropulsations. In particular, as extensively discussed by Schmucker (1985), the skin effect observed in the Meyer experiment (coupled with simultaneous measurements of the surface electric field) gave important information on the electrical structure of the recording area. Borehole magnetic measurements conducted up to depths of 3000 m (Spitzer, 1993) have also shown that impedances derived from the observed skin effect are much less distorted by shallow conductivity inhomogeneities than standard magnetotelluric impedances.

In a recent paper, Patella and Siniscalchi (1994) discussed from a theoretical point of

---

*Mailing address:* Dr. Massimo Vellante, Dipartimento di Fisica, Università dell'Aquila, Via Vetoio 10, 67010 Coppito, L'Aquila, Italy; e-mail: vellante@aquila.infn.it

view (see also Jones, 1983a) the practical possibilities of this technique, investigating, in the framework of the standard magnetotelluric theory and for a horizontally layered Earth, the properties of an apparent resistivity function as determined from two-level measurements of the horizontal magnetic field variations.

In this paper, two additional apparent resistivity functions are introduced which may provide useful information for the interpretation of experimental results.

In addition, the possibility of measuring the attenuation of the magnetic vertical component of an horizontally varying source field is also taken into account, and it is shown that such a measurement can provide further indications of the underlying conductivity distribution, as well as a way for estimating the average conductivity of the layer between the two levels.

## 2. Apparent resistivity

Experimental results from magnetotelluric sounding methods are often expressed in terms of the frequency-dependent apparent resistivity defined by (Cagniard, 1953):

$$\rho_a^{\text{MT}}(\omega) = |\zeta_{xy}(\omega)|^2 / \mu_o \omega \quad (2.1)$$

where  $\mu_o$  is the magnetic permeability of free space and  $\zeta_{xy}(\omega) = E_x(\omega)/H_y(\omega)$  is the wave impedance expressed by the ratio between the complex amplitudes of the electric field  $E_x$  and the magnetic field intensity  $H_y$  measured at the Earth's surface along two perpendicular horizontal directions  $x, y$ . More generally,  $\zeta_{xy}(\omega)$  is the element of a tensor relating the horizontal components of the electric and magnetic wave field. For a plane electromagnetic wave diffusing vertically into a uniform half-space, the apparent resistivity is frequency independent and coincident with the actual resistivity of the medium. In the real situation, a model of the underground resistivity distribution, which depends on a certain number of free parameters (such as thickness and resistivity of different underground layers in 1D models), is proposed by determining the free parameters which pro-

vide the best agreement between theoretical and experimental behaviors.

An analogous apparent resistivity function, which is appropriate for the two-level magnetovariational method, was defined by Patella and Siniscalchi (1994) in terms of the ratio between the magnetic field components along a given horizontal direction ( $x$ ) measured at two different depths ( $z_1, z_2 = z_1 + d$ ):

$$\rho_a^{\text{MV}}(\omega) = j \mu_o \omega d^2 \ln^{-2} [H_x(z_2, \omega) / H_x(z_1, \omega)] \quad (2.2)$$

where  $j$  is the imaginary unit. This function also provides the actual resistivity in case of a uniform medium, while for more general resistivity distributions it exhibits a frequency behavior different from  $\rho_a^{\text{MT}}(\omega)$ .

The experimental evaluation of eq. (2.2) requires the estimation of both gain  $G_x(\omega)$  and phase  $\varphi_x(\omega)$  of the transfer function  $A_x(\omega) = H_x(z_2, \omega) / H_x(z_1, \omega)$ . We find it then useful to rewrite eq. (2.2) in a form showing the explicit dependence on these parameters. As a matter of fact, putting  $[H_x(z_2, \omega) / H_x(z_1, \omega)] = G_x(\omega) e^{j\varphi_x(\omega)}$  and omitting the dependence on frequency, we obtain

$$|\rho_a^{\text{MV}}| = \frac{\mu_o \omega d^2}{\ln^2 G_x + \varphi_x^2} \quad (2.3)$$

$$\text{Arg}(\rho_a^{\text{MV}}) = \tan^{-1} \left( \frac{\ln^{-2} G_x - \varphi_x^2}{2 \varphi_x \ln G_x} \right). \quad (2.4)$$

The two quantities  $\varphi_x$  and  $\ln G_x$  which appear in eqs. (2.3) and (2.4) are usually affected by approximately equal statistical errors (Bendat and Piersol, 1971). However, they may be affected by different bias errors: for instance,  $G_x$  may be biased downward by the presence of noise in the input measurements while  $\varphi_x$  may be biased by time synchronization error ( $\Delta t$ ) between sites ( $\Delta\varphi_x = \omega\Delta t$ ). We find it then useful to introduce two additional definitions of apparent resistivity  $\rho_a^G$  and  $\rho_a^\varphi$ , respectively depending on the gain and phase of the transfer

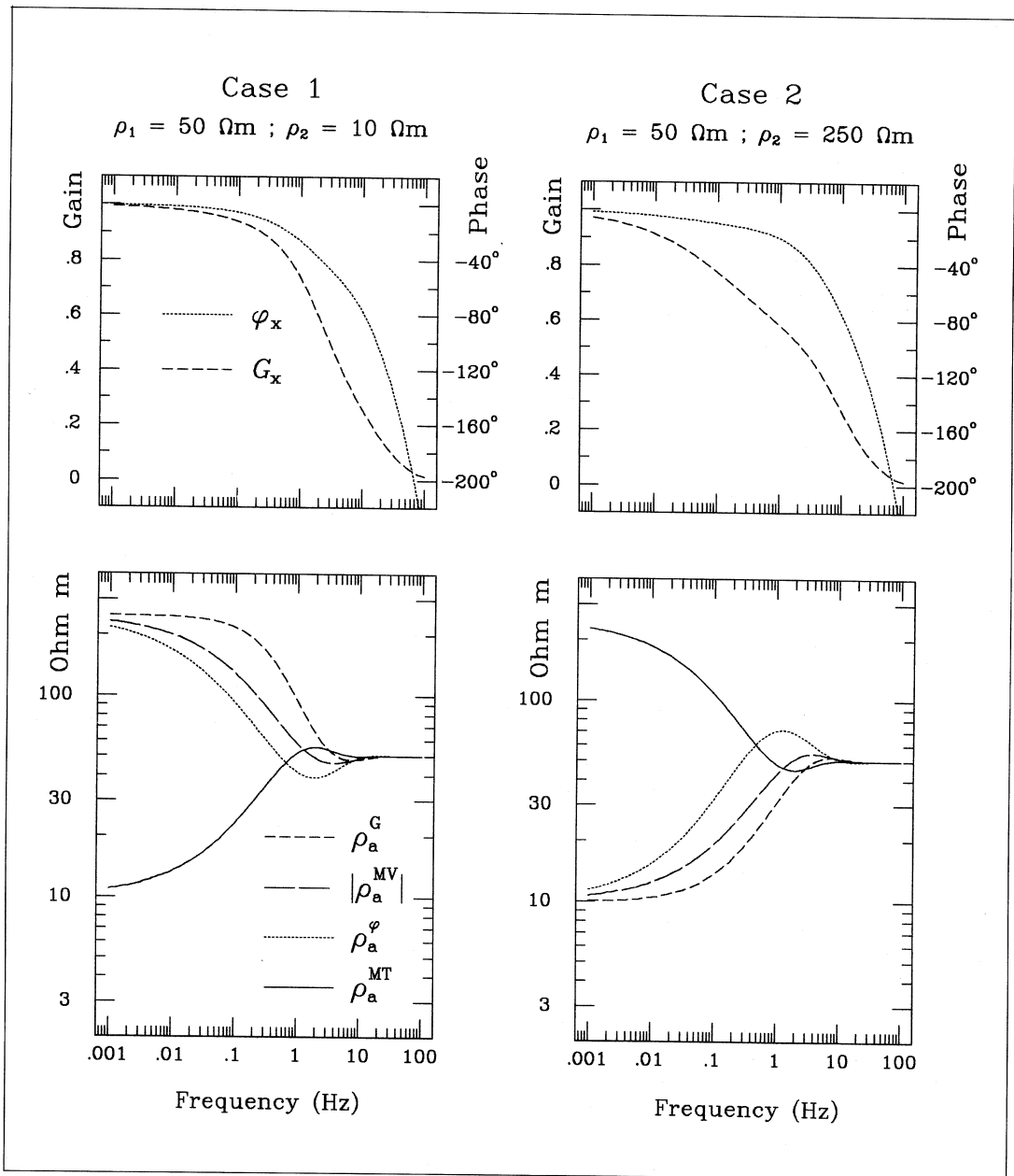


**Fig. 1.** Top panels: frequency behaviour of gain and phase (with respect to the surface) of the underground horizontal magnetic field for two different two-layer Earth models; a thickness of 3000 m for the first layer and a depth of 1500 m for the underground level have been assumed in both cases. Bottom panels: the corresponding behaviour of the magnetovariational apparent resistivity functions; the behaviour of the magnetotelluric apparent resistivity function is also shown.

function  $A_x$ , namely

$$\rho_a^G = \frac{\mu_o \omega d^2}{2 \ln^2 G_x} \quad (2.5)$$

$$\rho_a^p = \frac{\mu_o \omega d^2}{2 \varphi_x^2} \quad (2.6)$$

which derive straightforwardly from the uniform half-space case where  $\varphi_x = \ln G_x$  at all frequencies. From previous definitions it follows that

$$1/|\rho_a^{MV}| = (1/\rho_a^G + 1/\rho_a^p)/2 \quad (2.7)$$

*i.e.*, the absolute value of the apparent conductivity defined by Patella and Siniscalchi (1994) is the average of the two apparent conductivities given by eqs. (2.5) and (2.6).

In order to illustrate the frequency behaviour of the different apparent resistivity functions, we consider in fig. 1 two different two-layer Earth models:  $\rho_1 = 50 \Omega \cdot \text{m}$ ,  $h_1 = 3000 \text{ m}$ ,  $\rho_2 = 10 \Omega \cdot \text{m}$ ,  $h_2 = \infty$  (case 1), and an opposite situation in case 2 (second layer less conductive than the first layer:  $\rho_2 = 250 \Omega \cdot \text{m}$ , all other parameters being the same). The levels of the two measuring points have been assumed to be at the Earth's surface ( $z_1 = 0$ ) and at a depth  $z_2 = d = 1500 \text{ m}$ . On the top panels we show the frequency behaviour of both gain and phase of the transfer function  $A_x$  and on the bottom panels we show  $\rho_a^{MT}$ ,  $|\rho_a^{MV}|$ ,  $\rho_a^G$ ,  $\rho_a^p$ . As expected, all apparent resistivity functions provide the resistivity of the surface layer at high frequencies. At low frequencies, while the magnetotelluric function tends asymptotically to the resistivity of the second layer, the magnetovariational functions tend to a value which can be shown to be equal to  $\rho_1^2/\rho_2$  (this asymptotic behaviour for  $\rho_a^{MV}$  was derived analytically by Patella and Siniscalchi, 1994). It is worth noting that in the low frequency range ( $< 0.1 \text{ Hz}$ )  $\rho_a^p$  varies faster than  $\rho_a^G$ ; in magnetovariational experiments conducted at depths of few kilometers in the micropulsation band, like those reported by Meyer (1986) and Spitzer (1993),  $\rho_a^p$  would be then a more sensitive indicator (with respect to

$\rho_a^G$ ) of the underlying conductivity structure. In this same frequency range, the two opposite cases can be also distinguished by comparing  $\rho_a^G$  and  $\rho_a^p$  ( $\rho_a^G$  is greater or less than  $\rho_a^p$  depending whether the more conductive layer is the second or the first, respectively).

### 3. Effects of a finite wavelength of the source field

In the previous section we adopted the basic assumption in magnetotelluric theory (Cagniard, 1953) of a horizontally uniform source field. Wait (1954) and Price (1962) showed that the source field structure should be taken into account in the magnetotelluric method when the horizontal scale length of the variations becomes comparable to the skin depth of the signal in the Earth. It can be then important to investigate such effects also in the framework of the two-level magnetovariational method. For instance, since an arbitrary source also generates a vertical component of the magnetic field, it can be useful to study also the depth dependence of this component which, except for the uniform half-space case, is generally different from that of the horizontal component.

This can be done by adopting the approach of Price (1962) who showed that, inside a horizontally stratified Earth, the electric and magnetic fields resulting from an inducing source of arbitrary distribution can be built up from elementary solutions of form

$$E = \left( Q \frac{\partial P}{\partial y}, -Q \frac{\partial P}{\partial x}, 0 \right) e^{j\omega t} \quad (3.1)$$

$$H = \frac{j}{\mu_o \omega} \left( \frac{dQ}{dz} \frac{\partial P}{\partial x}, \frac{dQ}{dz} \frac{\partial P}{\partial y}, v^2 Q P \right) e^{j\omega t}. \quad (3.2)$$

In these expressions  $Q$  is a function only of the depth  $z$  and within each layer ( $n$ ) satisfies the Helmholtz equation:

$$\frac{d^2 Q}{dz^2} = k_n^2 Q \quad (3.3)$$

where  $k_n^2 = v^2 + j\mu_o \omega \sigma_n$ ,  $\sigma_n$  is the conductivity

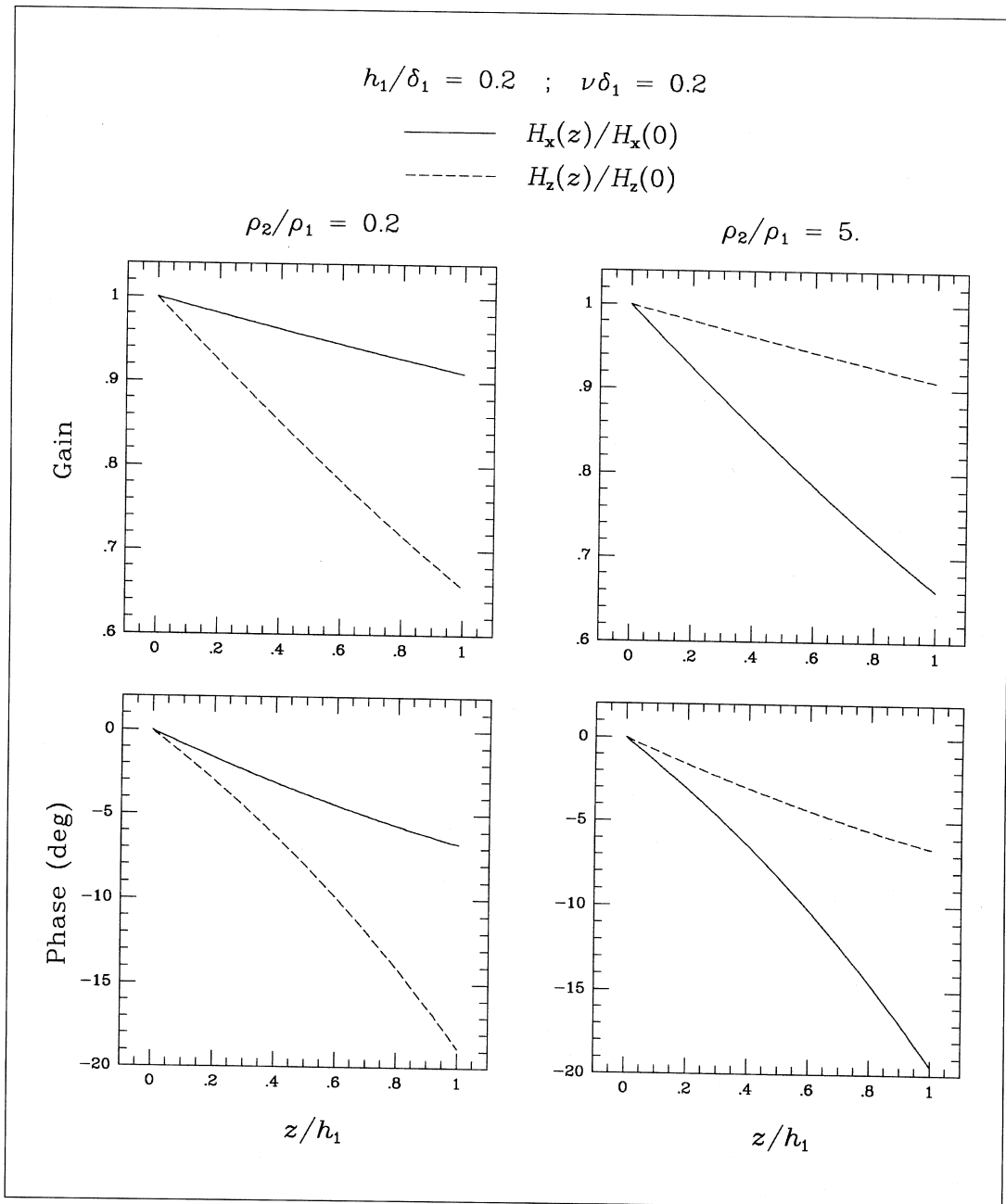


**Fig. 2a.** Gain and phase behaviour of the magnetic field components inside the first layer for two different two-layer Earth models; the ratio  $h_1/\delta_1$  between the thickness and the skin depth of the first layer, and the product  $\nu\delta_1$  between the horizontal wave number and the skin depth of the first layer have been both set equal to 0.2.

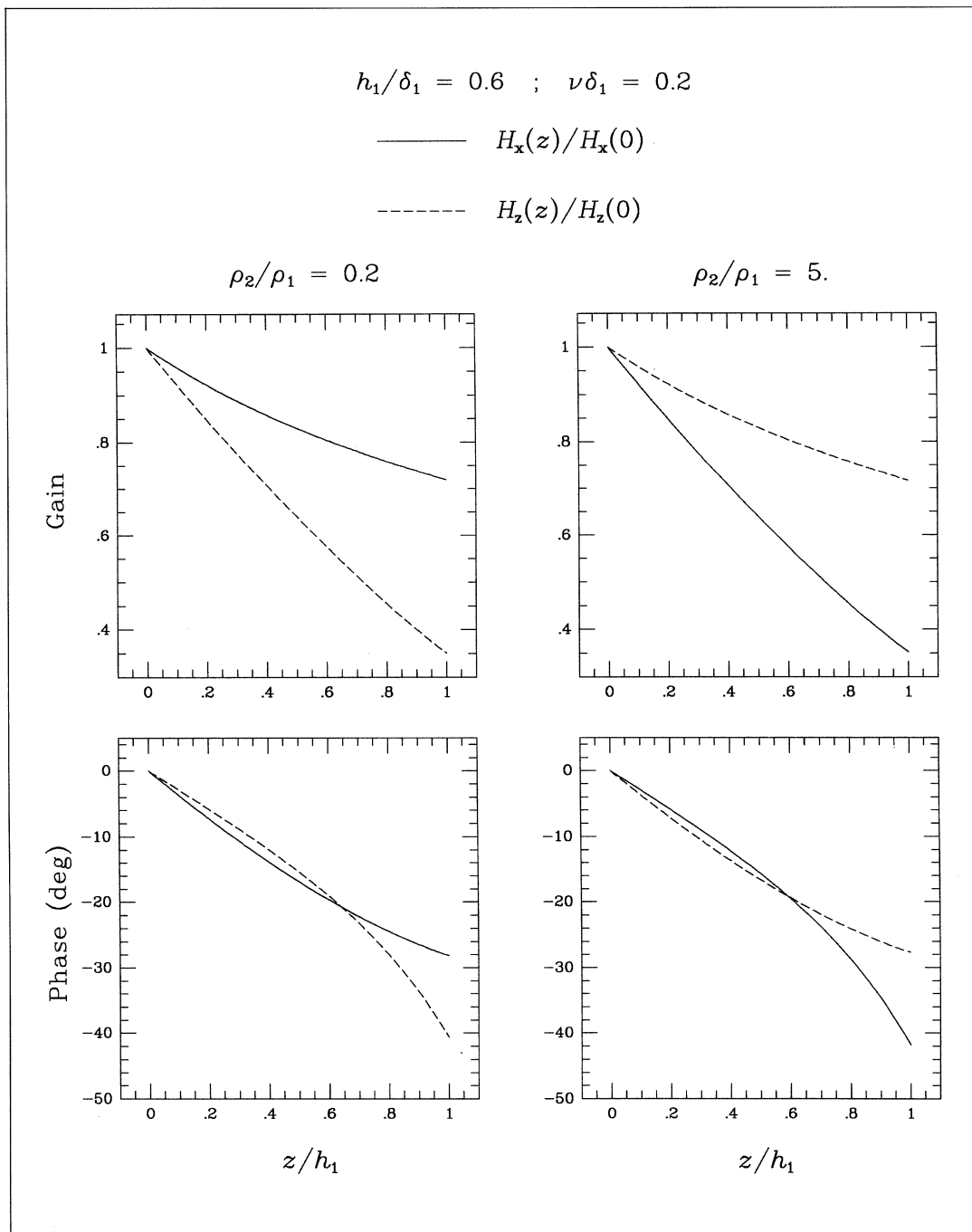


**Fig. 2b.** The same as fig. 2a but for  $h_1/\delta_1 = 0.6$ .

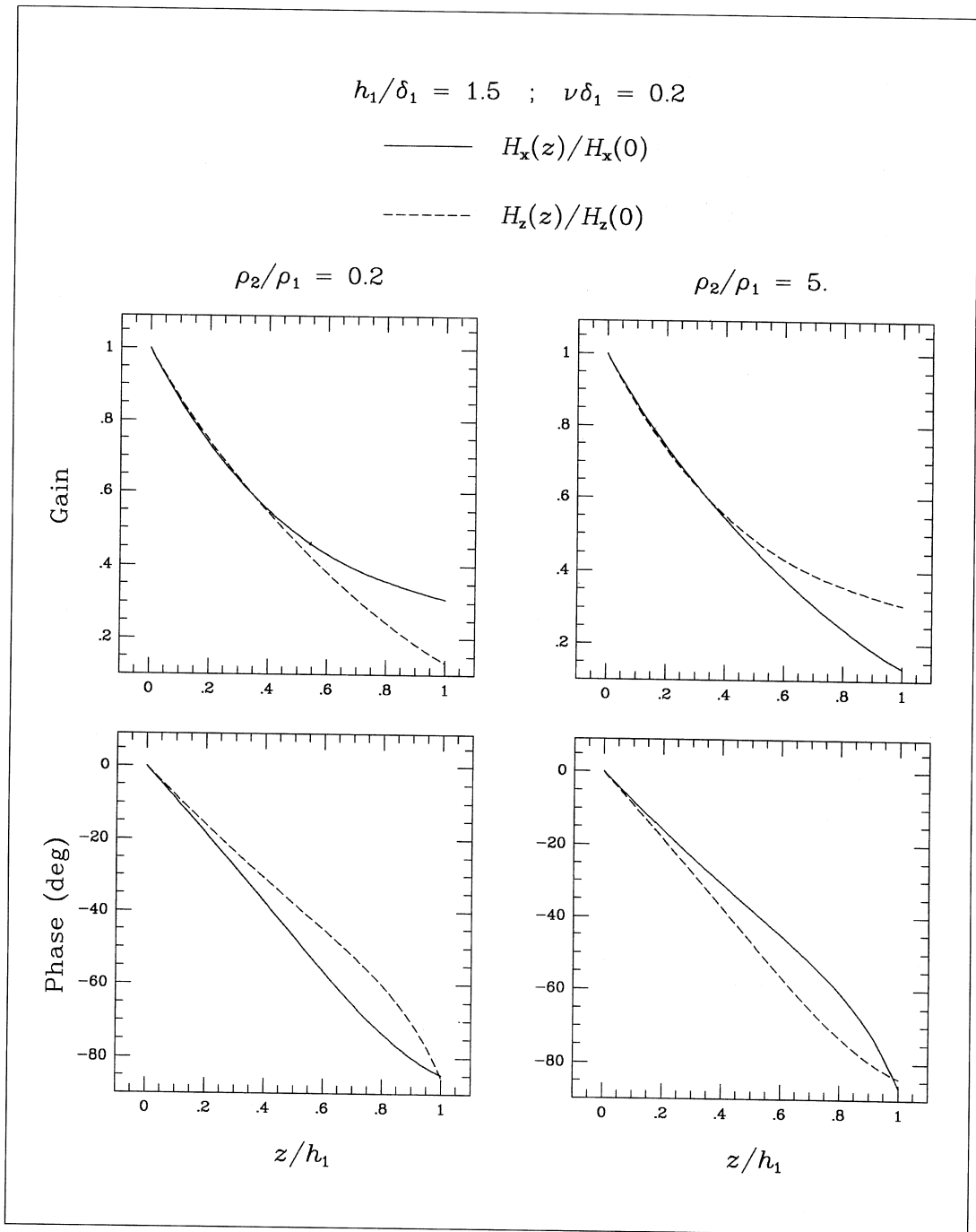


Fig. 2c. The same as fig. 2a but for  $h_1/\delta_1 = 1.5$ .

of the  $n^{\text{th}}$  layer, and  $v$  is a constant. The reciprocal of  $v$  is a measure of the horizontal scale length of the inducing field as shown by the equation governing the behaviour of the function  $P(x, y)$

$$\frac{\partial^2 P}{\partial x^2} + \frac{\partial^2 P}{\partial y^2} + v^2 P = 0. \quad (3.4)$$

By requiring the field components to be continuous across each layer interface and to tend to zero as  $z \rightarrow \infty$ , it is possible to obtain the depth dependence for any particular  $v$  value. The solutions for the horizontal components have the same form as those obtained in the standard magnetotelluric theory where the wave number  $k_n = (j\mu_o \omega \sigma_n)^{1/2}$  is replaced by the quantity  $(v^2 + j\mu_o \omega \sigma_n)^{1/2}$ . For instance, for a two-layer model we easily obtain within the first layer ( $0 \leq z \leq h_1$ )

$$\frac{H_x(z)}{H_x(0)} = \frac{H_y(z)}{H_y(0)} = \frac{e^{-k_1 z} (1 - \gamma e^{-2k_1(h_1 - z)})}{1 - \gamma e^{-2k_1 h_1}} \quad (3.5)$$

$$\frac{H_z(z)}{H_z(0)} = \frac{e^{-k_1 z} (1 + \gamma e^{-2k_1(h_1 - z)})}{1 + \gamma e^{-2k_1 h_1}} \quad (3.6)$$

where  $\gamma = (1 - k_2/k_1)/(1 + k_2/k_1)$ .

Price (1967) discussed only the particular case of a two-layer medium consisting of an ocean and a much less conductive substratum and showed that the vertical component throughout the first layer experiences a smaller attenuation than the horizontal component.

In order to provide useful indications for two-level magnetovariational measurements, we consider a two-layer model under more general conditions. Figures 2a-c show some examples of the behaviour (amplitude and phase) of both the horizontal and the vertical component inside the first layer. The different figures refer to different values of the ratio between the thickness  $h_1$  and the skin depth  $\delta_1 = (2/\mu_o \omega \sigma_1)^{1/2}$  of the first layer. In each example we assume a moderate horizontal variation of the field ( $v\delta_1 = 0.2$ ) and we consider,

as in the previous section, two opposite distributions of the underground electrical resistivity:  $\eta = \rho_2/\rho_1 = 0.2$  and  $\eta = 5$ . Note that in all examples there is an exchange of the depth profile between the two components when moving from the case  $\eta = 0.2$  to the case  $\eta = 5$ . This feature follows immediately from eqs. (3.5) and (3.6), as the  $\gamma$  parameter satisfies the property:  $\gamma(1/\eta) \equiv -\gamma(\eta)$  when  $v\delta_1 \ll 1$ . In particular, the first example (fig. 2a) shows that larger attenuations and phase delays are experienced by the horizontal or the vertical component depending on whether the more conductive layer is the first or the second, respectively. In the intermediate case (fig. 2b) these features still hold inside the whole first layer for the gain, but only beyond  $\sim 0.6 h_1$  for the phase. In the last case (fig. 2c) the gain curves begin to diverge at  $z/h_1 \equiv 0.4$  and, in contrast to the first case, the component with the larger phase delay is  $H_x$  when  $\eta = 0.2$  and  $H_z$  when  $\eta = 5$ .

These features are better illustrated in fig. 3 where phase and gain values of the two components are compared as a function of  $h_1/\delta_1$  and  $z/h_1$ . As can be seen, four regions with different characteristics can be identified. It must be pointed out, however, that in the top region of both panels the differences between vertical and horizontal components are very small (as in the range  $0 < z/h_1 < 0.4$  in fig. 2c). In this region, indeed, the conditions of a depth level far from the layer interface and  $h_1/\delta_1 > 1$ , make the signal attenuation similar to that of a uniform half-space.

The results of fig. 3 refer to two particular resistivity distributions and a particular  $v\delta_1$  value. More general results are shown in fig. 4 where different  $\rho_2/\rho_1$  values (curve labels) and two different  $v\delta_1$  values are considered. As in fig. 3, the solid and dashed curves represent contour lines where  $G_z = G_x$  and  $\varphi_z = \varphi_x$ , respectively. It can be noted that the  $\varphi_z = \varphi_x$  contour lines are much more dependent on the resistivity structure of the medium.

Let us now examine the effects of a finite source wavelength on the apparent resistivities defined by eqs. (2.1), (2.3), (2.5) and (2.6). Using the elementary solutions of Price (eqs. (3.1), (3.2) and (3.3)), we easily obtain in the case of



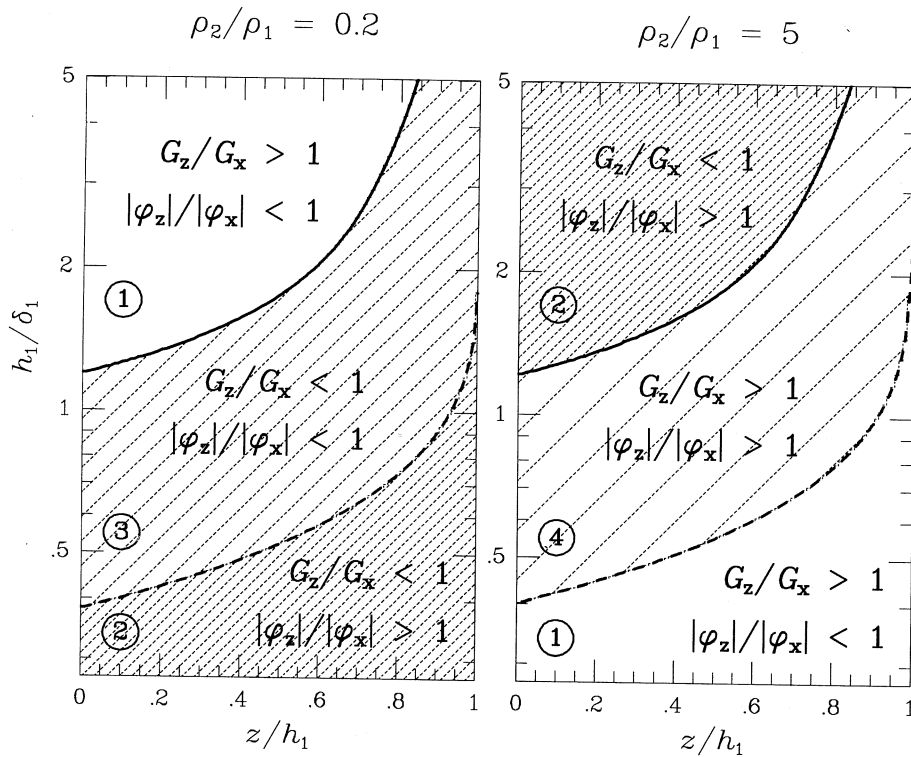


Fig. 3. Gain and phase comparison between  $H_z$  and  $H_x$  within the top layer of a two-layer medium with  $\rho_2/\rho_1 = 0.2$  (left) and  $\rho_2/\rho_1 = 5$  (right).  $v\delta_1 = 0.2$  in both cases.

a medium of uniform resistivity  $\rho$

$$\rho_a^G = \rho \left\{ \left[ 1 + \frac{1}{4} (v\delta)^4 \right]^{1/2} + \frac{1}{2} (v\delta)^2 \right\}^{-1} \quad (3.7)$$

$$\rho_a^\phi = \rho \left\{ \left[ 1 + \frac{1}{4} (v\delta)^4 \right]^{1/2} - \frac{1}{2} (v\delta)^2 \right\}^{-1} \quad (3.8)$$

$$|\rho_a^{MV}| = \rho_a^{MT} = \rho \left[ 1 + \frac{1}{4} (v\delta)^4 \right]^{-1/2}. \quad (3.9)$$

estimate. For small values of the parameter  $v\delta$  we obtain at a first order of approximation

$$\rho_a^G \cong \rho \left[ 1 - \frac{1}{2} (v\delta)^2 \right] \quad (3.10)$$

$$\rho_a^\phi \cong \rho \left[ 1 + \frac{1}{2} (v\delta)^2 \right] \quad (3.11)$$

$$|\rho_a^{MV}| = \rho_a^{MT} \cong \rho \left[ 1 - \frac{1}{8} (v\delta)^4 \right]. \quad (3.12)$$

It follows that  $\rho_a^G$ ,  $|\rho_a^{MV}|$ ,  $\rho_a^{MT}$  all provide downward biased estimates of the medium resistivity  $\rho$ , while  $\rho_a^\phi$  provides an upward biased

These expressions show that small departures from the plane wave approximation affect  $\rho_a^G$  and  $\rho_a^\phi$  much more than  $|\rho_a^{MV}|$  and  $\rho_a^{MT}$ . It is

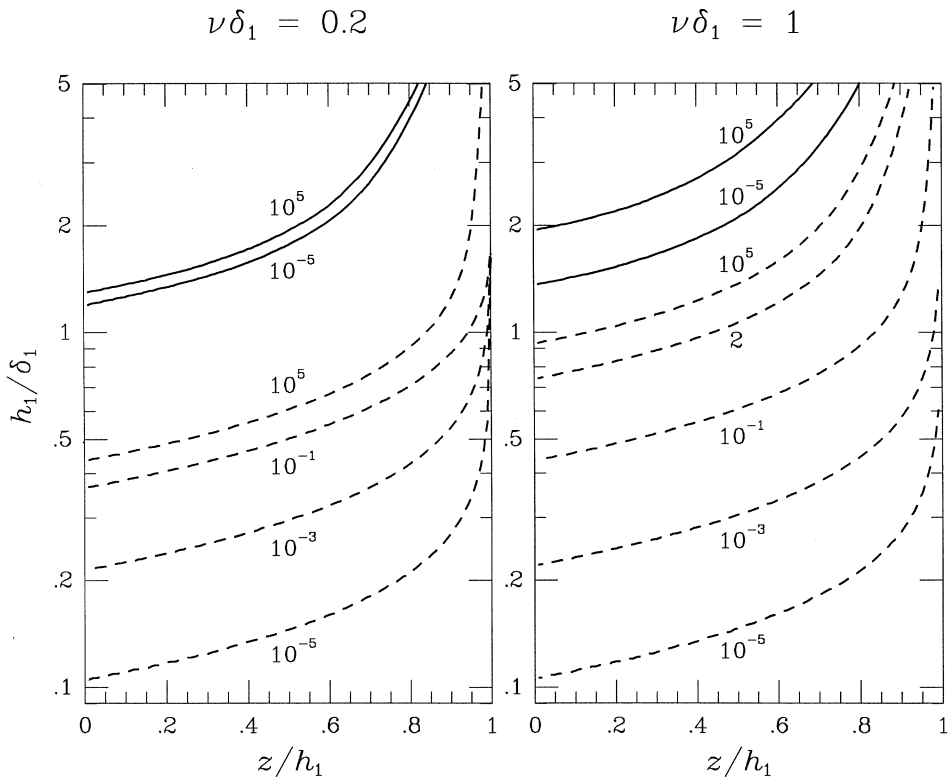


**Fig. 4.** Contour lines where  $G_z = G_x$  (solid lines) and  $\varphi_z = \varphi_x$  (dashed lines) within the top layer of different two-layer models. Curve labels indicate the ratio  $\rho_2/\rho_1$ .

however interesting to note that from eqs. (3.7) and (3.8), it follows

$$\rho_a^* = (\rho_a^G \rho_a^\phi)^{1/2} = \rho \quad (3.13)$$

*i.e.*, we obtain a new function  $\rho_a^*$  which provides the real resistivity of a uniform medium regardless of the  $\nu$  value.

For more general resistivity distributions in the medium, source field effects may be very different. As an example, we show in fig. 5 the behaviour of all apparent resistivities as a function of  $h_1/\delta_1$  for two different two-layer models ( $\rho_2/\rho_1 = 0.2$ , and  $\rho_2/\rho_1 = 5$ ). We also set  $\nu\delta_1 = 0.5$  and computed  $\rho_a^G$ ,  $\rho_a^\phi$ ,  $|\rho_a^{MV}|$  and  $\rho_a^*$  by assuming the first measuring point at the Earth's surface and the second one at the cen-

ter of the top layer ( $d/h_1 = 0.5$ ). All apparent resistivity functions have been scaled by the value corresponding to the plane wave approximation ( $\nu = 0$ ). As it can be seen, the effects of a finite  $\nu$  value are generally much greater on  $\rho_a^G$  and  $\rho_a^\phi$ . When  $\rho_2/\rho_1 = 0.2$ ,  $\rho_a^G$  and  $\rho_a^\phi$  (as for the uniform half-space case) are respectively smaller and greater than the values corresponding to  $\nu = 0$ . In the other case ( $\rho_2/\rho_1 = 5$ ), for small  $h_1/\delta_1$  values, the biases of  $\rho_a^G$  and  $\rho_a^\phi$  become opposite. Note that there are even particular conditions (in this example:  $h_1/\delta_1 \cong 1$  for  $\rho_a^\phi$ , and  $h_1/\delta_1 \cong 0.5$  for  $\rho_a^G$ ) when the finite  $\nu$  value has no effect on the apparent resistivity value. Significant effects can now be seen also on  $\rho_a^*$ , which generally has a bias of the same order of those of  $|\rho_a^{MV}|$  and  $\rho_a^{MT}$ .

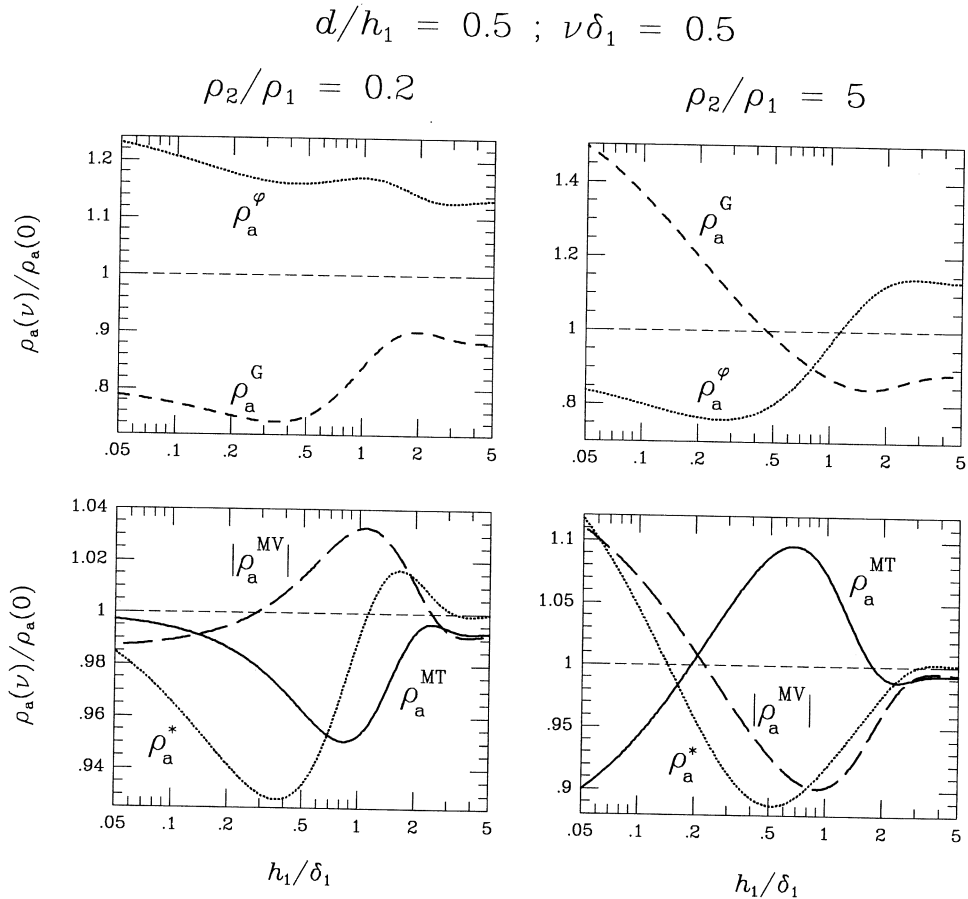


Fig. 5. Effects of a finite source wavelength ( $\nu\delta_1 = 0.5$ ) on the apparent resistivities in case of two-layer models.

#### 4. Estimation of the resistivity of the interlying medium

It will be shown now that the general solution of the magnetic field inside a plane layered half space (eq. (3.2)) also provides the possibility to estimate the resistivity of a given layer when two-level magnetovariational measurements are made inside the same layer. According to eqs. (3.2) and (3.3) each component  $\alpha = x, y, z$  of any particular mode of the magnetic field has a  $z$ -dependence within each layer (characterized by a conductivity  $\sigma$ )

such as

$$H_\alpha(z) = a_\alpha e^{kz} + b_\alpha e^{-kz} \quad (4.1)$$

where  $k = (\nu^2 + j\mu_o \omega \sigma)^{1/2}$ .

Let us consider, within the same layer, two measuring points of coordinates  $(x_o, y_o, z_o)$  and  $(x_o, y_o, z_o + d)$ , respectively. We can express each component of the magnetic field at  $z = z_o + d$  in terms of a Taylor series as follows

$$H_\alpha(z_o + d) = \sum_{m=0}^{\infty} \frac{d^m}{m!} H_\alpha^{(m)}(z_o) \quad (4.2)$$

where  $H_\alpha^{(m)}$  denotes the derivative of order  $m$  of  $H_\alpha$  with respect to  $z$ . Taking advantage of the following property

$$H_\alpha^{(m)} = \begin{cases} k^m H_\alpha^{(0)} & \text{for even } m \\ k^{m-1} H_\alpha^{(1)} & \text{for odd } m \end{cases} \quad (4.3)$$

we easily obtain

$$\begin{aligned} k[H_\alpha(z_0 + d) - H_\alpha(z_0) \cosh(kd)] &= \\ &= H_\alpha^{(1)}(z_0) \sinh(kd). \end{aligned} \quad (4.4)$$

We also get from eqs. (3.2) and (3.3)

$$H_x^{(1)}(z_0) H_z^{(1)}(z_0) = k^2 H_x(z_0) H_z(z_0). \quad (4.5)$$

Taking  $\alpha = x$  and  $z$  in eq. (4.4), and using eq. (4.5) we get after a few simple steps

$$\cosh(kd) = \frac{H_x(z_0) H_z(z_0) + H_x(z_0 + d) H_z(z_0 + d)}{H_x(z_0) H_z(z_0 + d) + H_x(z_0 + d) H_z(z_0)} \quad (4.6)$$

which relates the parameter  $k$  to the magnetic field values at two positions within the same layer. In terms of the conductivity we get after inverting eq. (4.6)

$$\sigma = \frac{\ln^2 [w + (w^2 - 1)^{1/2}] - v^2 d^2}{j \mu_o \omega d^2} \quad (4.7)$$

where

$$\begin{aligned} w &= \frac{A_x A_z + 1}{A_x + A_z}; \quad A_x = \frac{H_x(z_0 + d)}{H_x(z_0)}; \\ A_z &= \frac{H_z(z_0 + d)}{H_z(z_0)}. \end{aligned} \quad (4.8)$$

We can now define from eq. (4.7)

$$\tilde{\sigma} = \frac{\ln^2 [w + (w^2 - 1)^{1/2}]}{j \mu_o \omega d^2} \quad (4.9)$$

which can be computed from two-level mea-

surements and is related to the actual conductivity  $\sigma$  by the following expression

$$\tilde{\sigma} = \sigma \left( 1 - j \frac{v^2}{\mu_o \omega \sigma} \right). \quad (4.10)$$

This expression shows that when the horizontal scale length  $1/v$  is large in comparison to the skin depth  $(2/\mu_o \omega \sigma)^{1/2}$  in the layer,  $\tilde{\sigma}$  approximates the real conductivity whatever the conductivity of the other layers is. It is also worth noting that for any single wave mode the real part of  $\tilde{\sigma}$  coincides with  $\sigma$ , no matter how large  $v$  is. Strictly speaking, this is no longer true when real source fields with a continuous spectrum of elementary wave modes are considered. We can expect however that, when the main contribution to the source field comes from wave modes whose wavelength is significantly larger than the skin depth (as for most natural sources)  $\text{Re}(\tilde{\sigma})$  still provides a good estimate of  $\sigma$ . A numerical example is given in the next section.

### 5. A numerical example

In order to test the theoretical results of the previous section in a realistic case, we consider a source field produced by a horizontal current sheet located at a height  $h = 120$  km above the Earth's surface (*i.e.*, at the height of the ionospheric E-layer); the surface current is assumed to flow along the  $y$  direction and to depend on the  $x$ -coordinate and time as follows:

$$K_y(x, t) = K_0 (1 - jx/\varepsilon)^{-1} e^{j\omega t}, \quad z = -h \quad (5.1)$$

where  $K_y$  is the current per unit length. The corresponding magnetic potential  $\Omega$  can be written in the form

$$\begin{aligned} \Omega &= j \varepsilon (K_0/2) e^{j\omega t} \int_0^\infty v^{-1} e^{-v(\varepsilon + h + z)} e^{jvx} dv, \\ &z > -h. \end{aligned} \quad (5.2)$$

On the Earth's surface ( $z = 0$ ) the primary field

associated with this source is

$$H_x(x, t) = (\epsilon K_0/2)(\epsilon + h - jx)^{-1} e^{j\omega t}, \quad z = 0 \quad (5.3)$$

$$H_z(x, t) = jH_x(x, t), \quad z = 0. \quad (5.4)$$

The expression (5.3) corresponds to the meridional profile of the geomagnetic pulsation field (N-S component) as predicted from the Field Line Resonance (FLR) theory (Southwood, 1974). This spatial structure has been confirmed by numerous observations at meridional arrays on the ground (Menk *et al.*, 1994).

According to eq. (5.3) the amplitude has a maximum at  $x = 0$ , *i.e.*, at the meridional coordinate of the foot of the magnetic field line whose resonant frequency matches the source frequency  $\omega$ . The quantity  $\epsilon + h$  represents the width of the resonance region on the ground and, for the present purpose, it can be simply considered a measure of the scale of variation of the source field. Assuming  $\epsilon = 80$  km we get  $\epsilon + h = 200$  km, in agreement with typically observed resonance widths (Menk *et al.*, 1994). We also assume for this numerical example a period wave  $T = 2\pi/\omega = 20$  s which corresponds to the typical resonant period obser-

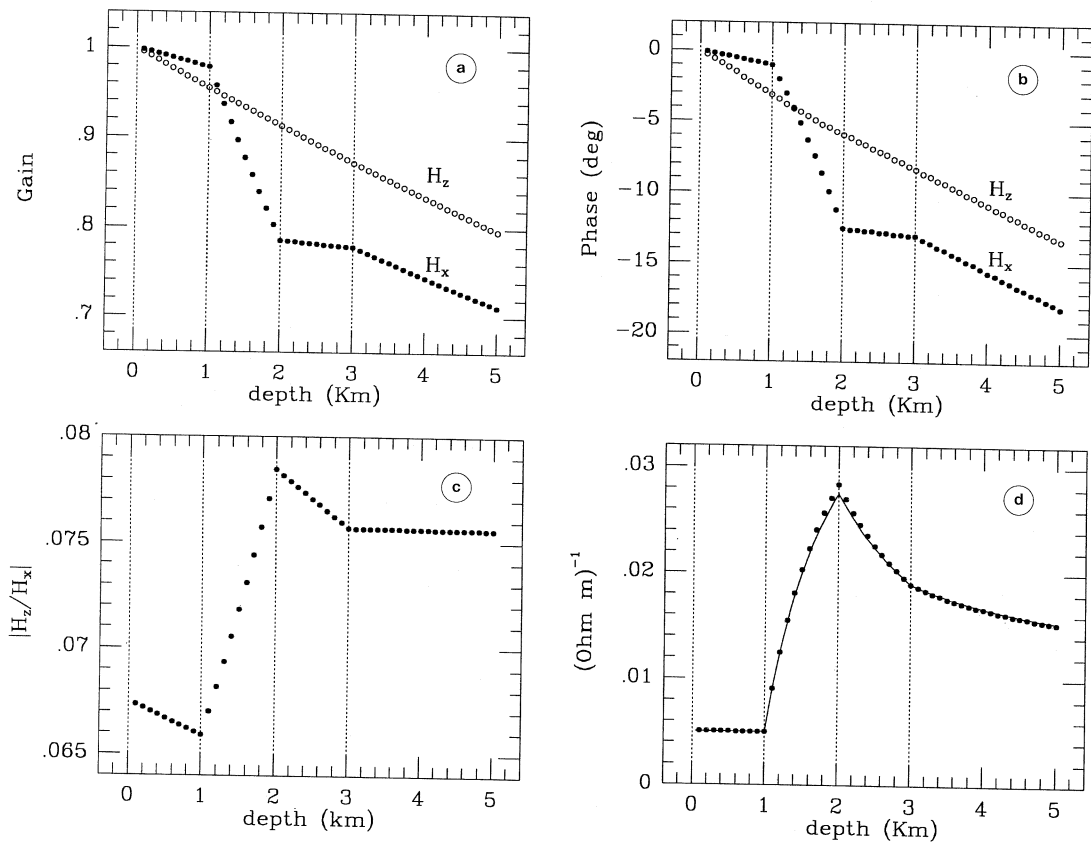


**Fig. 6a-d.** Numerical results of a model consisting of a time varying inhomogeneous current sheet above a 4-layer geoelectric structure: underground vertical profile of the amplitude (a) and phase (b) of the magnetic field;  $|H_z/H_x|$  ratio (c); real part of  $\tilde{\sigma}$  (dots) and average conductivity (continuous curve) are shown in panel (d).

ved at geomagnetic latitudes of  $\sim 45^\circ$  (Menk *et al.*, 1994).

The expression (5.2) of the magnetic potential of the inducing field allows the formalism described in section 3 to be used to obtain the field inside a horizontally stratified Earth by integrating the elementary solutions in the  $v$  domain (Price, 1967). As a matter of fact, for the present spatial field structure, it was sufficient to integrate in the interval  $0-1/20 \text{ km}^{-1}$ . The computation was made for the following 4-layer model:  $\rho_1 = 200 \Omega \cdot \text{m}$ ;  $h_1 = 1 \text{ km}$ ;  $\rho_2 = 20 \Omega \cdot \text{m}$ ;  $h_2 = 1 \text{ km}$ ;  $\rho_3 = 500 \Omega \cdot \text{m}$ ;  $h_3 = 1 \text{ km}$ ;  $\rho_4 = 100 \Omega \cdot \text{m}$ ;  $h_4 = \infty$ . The vertical profiles at  $x = 0$  of both  $H_x$  and  $H_z$  are shown in figs. 6a,b up to a depth of 5 km. Figure 6c shows the behaviour of the ratio  $|H_z/H_x|$ . Because of the large horizontal scale length with respect to the skin depth ( $(\varepsilon + h)/\delta \cong 10$ ), the vertical component turns out to be rather small:  $|H_z/H_x| \cong 0.07$ . The vertical profiles of  $H_x$  and  $H_z$  were finally used to compute  $\tilde{\sigma}$  (eq. (4.9)). The first measuring site was assumed to be at the Earth's surface ( $z_0 = 0$ ) and the second site at a depth  $d$  varying between 0.1 km and 5 km. In fig. 6d the dots correspond to the real part of  $\tilde{\sigma}$  and the continuous curve represents the quantity  $(1/d) \int_0^d \sigma(z) dz$ , *i.e.*, the average conductivity between the surface and the depth  $d$ . We can see that, as expected from the theoretical results of the previous section, when the two measuring points are within the same layer ( $d < 1 \text{ km}$ )  $\text{Re}(\tilde{\sigma})$  coincides with the layer conductivity; besides, when the interlying medium is not uniform ( $d > 1 \text{ km}$ )  $\text{Re}(\tilde{\sigma})$  provides a very good estimate of the average conductivity (the largest discrepancy,  $\cong 3\%$ , occurs at the interface between the second and third layer).

It must be remarked, however, that in the case of too small depths, this agreement can be purely theoretical because unavoidable noise contributions in the measurements may prevent the detection of small differences between surface and underground signals; for instance the maximum attenuation experienced by  $H_x$  and  $H_z$  in the first layer of the present example (2% and 4% respectively, fig. 6a) would be too small for a confident estimate of the layer conductivity. More significant attenuations would be obtained in more conductive structures or at

higher frequencies, but this would also cause a smaller vertical signal. It should also be pointed out that, due to its relatively short wavelength, the source field generated by the FLR mechanism probably represents the best case for the present method. Therefore, for a practical use of this technique, a careful selection of events characterized by strong FLR effects is required.

## 6. Summary and discussion

In this paper we have discussed some theoretical aspects of the two-level magnetovariational method for the determination of the underground electrical structure. In particular we have introduced two useful apparent resistivity functions  $\rho_a^G$  and  $\rho_a^\phi$ , respectively depending on gain and phase of the transfer function of the horizontal magnetic field between the Earth's surface and a given depth. A similar function  $\rho_a^{\text{MV}}$ , depending on both gain and phase, was previously defined by Patella and Siniscalchi (1994). All these functions contain essentially the same information about the electrical properties of the medium, so in principle each of them can be used for modelling the underground electrical structure. However, in case one of the two parameters (gain or phase) is not well determined, the present double definition of apparent resistivity gives the opportunity to use a function depending only on the best determined parameter. On the other hand, we also found that  $\rho_a^{\text{MV}}$  is usually much less affected by a finite wavelength in the source field.

We have also investigated, for a two-layer Earth model, the behaviour of a vertical magnetic field generated by a source of finite wavelength determining the conditions for which this component inside the top layer is more or less attenuated (or phase delayed) than the horizontal component.

Lastly, we have suggested a method for determining the conductivity of a uniform layer from the measurements of the horizontal and vertical magnetic field variations at two levels inside the layer. We have also shown in a real-

istic source field example that when the conductivity varies within the two levels a very good estimate of the depth-integrated conductivity of the interlying medium can be obtained. The possibility to obtain an estimate of the conductance of the «roof rock» in mines was already proposed by Schmucker (unpublished report, 1985) who considered, however, measurements of the surface electric field instead of two-level measurements of the vertical magnetic field.

The measurement of the attenuation of the vertical component is not a simple task because, for typical conditions, this component is quite small and the effect of the source field can be masked by anomalous fields produced by lateral variations of the Earth's conductivity (Gough and Ingham, 1983). There have been, however, several cases in the past where, assuming a negligible anomalous field, surface measurements of this component were used (together with measurements of the horizontal gradients of the horizontal magnetic field) to provide alternative estimates of the wave impedance (Connerney and Kuckes, 1980; Lilley *et al.*, 1981; Jones, 1983b). In case the anomalous field cannot be neglected, its contribution can still be reduced as proposed by Cochrane and Hyndman (1970) and Lilley and Sloane (1976).

### Acknowledgements

The author thanks Prof. U. Villante for critical readings of the manuscript and helpful suggestions and Prof. D. Patella for useful discussions. This work was supported by MURST (40%-04 contract).

### REFERENCES

BABOUR, K. and J. MOSNIER (1980): Direct determination of the characteristics of the currents responsible for the geomagnetic anomaly of the Rhinegraben, *Geophys. J. R. Astron. Soc.*, **60**, 327-331.  
 BENDAT, J.S. and A.G. PIERSOL (1971): *Random Data: Analysis and Measurement Procedures* (Wiley-Interscience, New York), pp. 407.  
 BERDICHEVSKII, M.N. and L.L. VANYAN (1969): Perspec-

tives of magnetotelluric sounding at sea (in Russian), *Fizika Zemli*, **11**, 51-56.  
 CAGNIARD, L. (1953): Basic theory of the magnetotelluric method of geophysical prospecting, *Geophysics*, **18**, 605-635.  
 COCHRANE, N.A. and R.D. HYNDMAN (1970): A new analysis of geomagnetic depth-sounding data from Western Canada, *Can. J. Earth Sci.*, **7**, 1208-1218.  
 CONNERNEY, J.E.P. and A.F. KUCKES (1980): Gradient analysis of geomagnetic fluctuations in the Adirondacks, *J. Geophys. Res.*, **85**, 2615-2624.  
 EDWARDS, R.N., P.A. WOLFGAMM and A.S. JUDGE (1988): The ICE-MOSES experiment: mapping permafrost zones electrically beneath the Beaufort Sea, *Mar. Geophys. Res.*, **9**, 265-290.  
 GOUGH, D.I. and M.R. INGHAM (1983): Interpretation methods for magnetometer arrays, *Rev. Geophys. Space Phys.*, **21**, 805-827.  
 HARDAM, W. (1974): Direct determination of the skin effect based on recordings of geomagnetic pulsations above and underground, *Thesis*, Institute of Geophysics of the University of Gottingen.  
 JONES, A.G. (1983a): A passive natural-source twin-purpose borehole technique: Vertical Gradient Magnetometry (VGM), *J. Geomagn. Geoelect.*, **38**, 473-490.  
 JONES, A.G. (1983b): The electrical structure of the lithosphere and asthenosphere beneath the Fennoscandian shield, *J. Geomagn. Geoelect.*, **35**, 811-827.  
 KAUFMAN, A.A. and G.V. KELLER (1981): The magnetotelluric sounding method, *Methods in Geochemistry and Geophysics* (Elsevier, Amsterdam), vol. 15, pp. 595.  
 LAW, L.K. and J.P. GREENHOUSE (1981): Geomagnetic variation sounding of the asthenosphere beneath the Juan de Fuca Ridge, *J. Geophys. Res.*, **86**, 967-978.  
 LILLEY, F.E.M. and M.N. SLOANE (1976): On estimating electrical conductivity using gradient data from magnetometer arrays, *J. Geomagn. Geoelect.*, **28**, 321-328.  
 LILLEY, F.E.M., D.V. WOODS and M.N. SLOANE (1981): Electrical conductivity from Australian magnetometer arrays using spatial gradient data, *Phys. Earth Planet. Inter.*, **25**, 202-209.  
 MENK, F.W., B.J. FRASER, C.L. WATERS, C.W.S. ZIESOLECK, Q. FENG, S.H. LEE and P.W. MCNABB (1994): Ground measurements of low latitude magnetospheric field line resonances, in *Solar Wind Sources of Magnetospheric Ultra-Low-Frequency Waves*, *Geophysical Monograph 81*, edited by M.J. ENGBRETSON, K. TAKAHASHI and M. SCHOLER, American Geophysical Union, 299-310.  
 MEYER, R. (1986): Direct determination of the skin effect, *Thesis*, Institute of Geophysics of the University of Gottingen.  
 PATELLA, D. and A. SINISCALCHI (1994): Two-level magnetovariational measurements for the determination of underground resistivity distributions, *Geophys. Prospect.*, **42**, 417-444.  
 POEHLIS, K.A. and R.P. VON HERZEN (1976): Electrical resistivity structure beneath the North-West Atlantic ocean, *Geophys. J. R. Astron. Soc.*, **47**, 331-346.  
 PRICE, A.T. (1962): The theory of magnetotelluric methods when the source field is considered, *J. Geophys. Res.*, **67**, 1907-1918.

- PRICE, A.T. (1967): Electromagnetic induction within the Earth, in *Physics of Geomagnetic Phenomena*, edited by S. MATSUSHITA and W.H. CAMPBELL (Academic Press, New York), vol. 1, 235-298.
- SOUTHWOOD, D.J. (1974): Some features of field line resonances in the magnetosphere, *Planet. Space Sci.*, **22**, 483-491.
- SPITZER, K. (1993): Observations of geomagnetic pulsations and variations with a new borehole magnetometer down to depths of 3000 m, *Geophys. J. Int.*, **115**, 839-848.
- WAIT, J.R. (1954): On the relation between telluric currents and the Earth's magnetic field, *Geophysics*, **19**, 281-289.
- (received November 6, 1996;  
accepted May 28, 1997)